Available online at www.sciencedirect.com
ScienceDirect
Journal of Power Sources 163 (2006) 151–157
JOURNAL OF POWER SOURCES
www.elsevier.com/locate/jpowsour

# A two-dimensional modeling of a lithium-polymer battery

Ki Hyun Kwon [a], Chee Burm Shin [a,*], Tae Hyuk Kang [b], Chi-Su Kim [b]

[a] *Ajou University, Department of Chemical Engineering, 5 Wonchun-Dong, Suwon 443-749, South Korea*
[b] *VK Corporation, Battery R&D Center, Pyeongtaek 450-090, South Korea*

Received 18 August 2005; received in revised form 18 February 2006; accepted 6 March 2006
Available online 18 April 2006

**Abstract**

The potential and current density distribution on the electrodes of a lithium-polymer battery were studied by using the finite element method. The effect of the configuration of the electrodes such as the aspect ratio of the electrodes and the size and placing of current collecting tabs as well as the discharge rates on the battery performance was examined to enhance the uniformity of the utilization of the active material of electrodes. The results showed that the aspect ratio of the electrodes and the size and placing of current collecting tabs have a significant effect on the potential and current density distribution on the electrodes to influence the distribution of the depth of discharge on the electrodes, thus affecting the uniform utilization of the active material of electrodes.


*Keywords:* Lithium-polymer battery; Model; Electrode configuration; Potential distribution; Current density distribution; Finite element method

## 1. Introduction

There is a significant interest in the use of batteries for hybrid electric vehicle (HEV) and electric vehicle (EV). The outstanding characteristics of lithium-polymer batteries (high energy density, high voltage, low self-discharge rate, and good stability among others) make them one of the preferred choices for such applications. However, much larger lithium-polymer batteries than those available in the market for consumer electronics are required for HEV and EV applications. The performance of a battery electrode is influenced by the aspect ratio, the placing of current collecting tabs, and the total amount of the current flowing through an electrode. If an electrode is not designed optimally, the potential and current density will be non-uniformly distributed, and the utilization of the active material over the electrode will be non-uniform. Accelerated degradation of the electrode may result due to excessive localized utilization of the active material on the electrode. That effect becomes more pronounced, as the size of the electrode becomes larger. Therefore, an optimum design of the electrode is pertinent for the production of large-scale lithium-polymer batteries.

When scaling up a small-scale cell to a large-scale battery, mathematical modeling plays an important role, because nearly limitless design iterations can be performed by using simulations [1]. Previous reviews of the modeling of lithium batteries are given in references [2–5]. A one-dimensional model assumes that the gradients of the variables adopted in modeling are negligible in the two directions parallel to the current collectors. Such an assumption may be valid for small-scale cells. However, that assumption may not be justified for large-scale batteries, since the potential drop along the current collector due to ohmic drop may be significant enough to affect the current distribution, with a higher current closer to the tabs. Then, a two- or three-dimensional model may be desirable for large-scale batteries [6–9].

In this work, a two-dimensional modeling is performed to calculate the potential and current density distribution on the electrodes of a lithium-polymer battery comprising a $LiMn_2O_4$ cathode, a graphite anode, and a plasticized electrolyte. This work adopts a relatively simpler modeling approach by considering only Ohm's law and charge conservation on the electrodes based on the simplified polarization characteristics of the electrodes as compared to the previously published papers by other researchers [10–15]. The distribution of the depth of discharge (DOD) on the electrode is predicted as a function of discharge time from the calculated potential and current density distribution. Based on the distribution of DOD, the effects of the aspect

* Corresponding author. Tel.: +82 31 219 2388; fax: +82 31 219 1612.
*E-mail address:* cbshin@ajou.ac.kr (C.B. Shin).

0378-7753/$ – see front matter © 2006 Elsevier B.V. All rights reserved.
doi:10.1016/j.jpowsour.2006.03.012

ratio of the electrodes, the size and placing of current collecting tabs, and discharge rates on the battery performance are evaluated.

## 2. Mathematical model

A schematic diagram of the current flow in the parallel plate electrodes of a battery is shown in Fig. 1. The distance between the electrodes is assumed to be so small that the current flow between the electrodes is perpendicular to the electrodes. From the continuity of current on the electrodes, the following equations can be derived:

$$\nabla \cdot \vec{i}_{\mathrm{p}} - J = 0 \quad \text{in } \Omega_{\mathrm{p}} \tag{1}$$

$$\nabla \cdot \vec{i}_{\mathrm{n}} + J = 0 \quad \text{in } \Omega_{\mathrm{n}} \tag{2}$$

where $\vec{i}_{\mathrm{p}}$ and $\vec{i}_{\mathrm{n}}$ are the linear current density vectors (current per unit length ($\mathrm{A\,cm^{-1}}$)) in the positive and negative electrodes, respectively, and $J$ is the current density (current per unit area ($\mathrm{A\,cm^{-2}}$)) transferred through the separator from the negative electrode to the positive electrode. $\Omega_{\mathrm{p}}$ and $\Omega_{\mathrm{n}}$ denote the domains of the positive and negative electrodes, respectively. By Ohm's law, $\vec{i}_{\mathrm{p}}$ and $\vec{i}_{\mathrm{n}}$ can be written as

$$\vec{i}_{\mathrm{p}} = -\frac{1}{r_{\mathrm{p}}}\nabla V_{\mathrm{p}} \quad \text{in } \Omega_{\mathrm{p}} \tag{3}$$

$$\vec{i}_{\mathrm{n}} = -\frac{1}{r_{\mathrm{n}}}\nabla V_{\mathrm{n}} \quad \text{in } \Omega_{\mathrm{n}} \tag{4}$$

where $r_{\mathrm{p}}$ and $r_{\mathrm{n}}$ are the resistances ($\Omega$) of the positive and negative electrodes, respectively, and $V_{\mathrm{p}}$ and $V_{\mathrm{n}}$ are the potentials (V) of the positive and negative electrodes, respectively. By substituting Eqs. (3) and (4) into Eqs. (1) and (2), the following Poisson equations for $V_{\mathrm{p}}$ and $V_{\mathrm{n}}$ are obtained:

$$\nabla^2 V_{\mathrm{p}} = -r_{\mathrm{p}} J \quad \text{in } \Omega_{\mathrm{p}} \tag{5}$$

$$\nabla^2 V_{\mathrm{n}} = +r_{\mathrm{n}} J \quad \text{in } \Omega_{\mathrm{n}} \tag{6}$$

The relevant boundary conditions for $V_{\mathrm{p}}$ are

$$\frac{\partial V_{\mathrm{p}}}{\partial n} = 0 \quad \text{on } \Gamma_{\mathrm{p}_1} \tag{7}$$

$$-\frac{1}{r_{\mathrm{p}}}\frac{\partial V_{\mathrm{p}}}{\partial n} = \frac{I_0}{L} \quad \text{on } \Gamma_{\mathrm{p}_2} \tag{8}$$

where $\partial/\partial n$ denotes the gradient in the direction of the outward normal to the boundary. The first boundary condition (7) implies that there is no current flow through the boundary ($\Gamma_{\mathrm{p}_1}$) of the electrode other than the tab. The second boundary condition (8) means that the linear current density through the tab ($\Gamma_{\mathrm{p}_2}$) of the length $L$ (cm) is constant to the value of $I_0/L$. $I_0$ is the total current (A) through the tab in the mode of constant-current discharge. The boundary conditions for $V_{\mathrm{n}}$ are

$$\frac{\partial V_{\mathrm{n}}}{\partial n} = 0 \quad \text{on } \Gamma_{\mathrm{n}_1} \tag{9}$$

$$V_{\mathrm{n}} = 0 \quad \text{on } \Gamma_{\mathrm{n}_2} \tag{10}$$

The first boundary condition (9) implies the same as in the case of $V_{\mathrm{p}}$. The second boundary condition (10) means that the potential at the tab of the negative electrode is fixed to the value of zero as the reference potential.

The resistance, $r$ ($r_{\mathrm{p}}$ or $r_{\mathrm{n}}$), is calculated as follows:

$$r = \frac{1}{h_{\mathrm{c}} S_{\mathrm{c}} + h_{\mathrm{e}} S_{\mathrm{e}}} \tag{11}$$

where $h_{\mathrm{c}}$ and $h_{\mathrm{e}}$ are the thicknesses (cm) of the current collector and the electrode material, respectively, and $S_{\mathrm{c}}$ and $S_{\mathrm{e}}$ are the electrical conductivities ($\mathrm{S\,cm^{-1}}$) of the current collector and the electrode material, respectively. The parameters used in the calculations of resistances for the electrodes are listed in Table 1. The values of electrical conductivities of composite electrodes are the same as those used in the references [14,15]. The current collectors of cathode and anode are made of aluminum and copper, respectively.

The current density, $J$, of Eqs. (5) and (6) is the function of the potential difference between the positive and negative electrodes, $(V_{\mathrm{p}} - V_{\mathrm{n}})$. The functional form depends on the polarization characteristics of the electrodes. In this study, the following

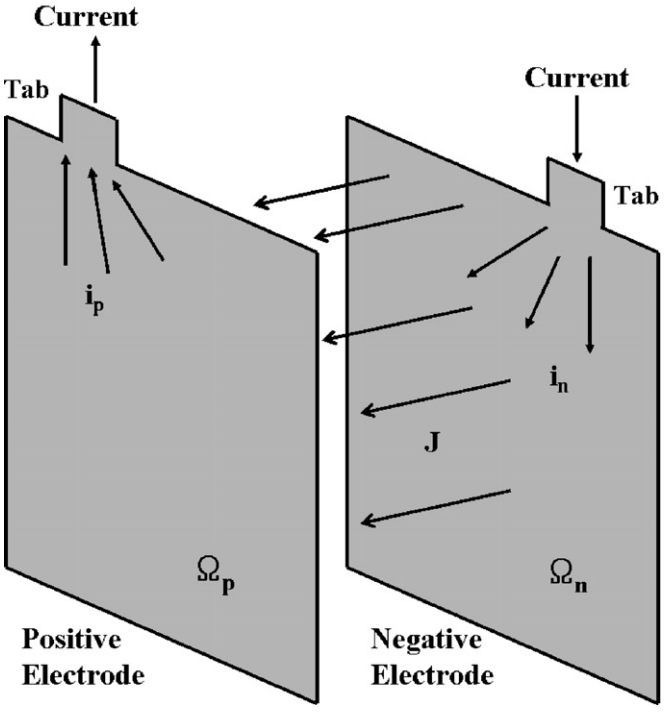


Fig. 1. Schematic diagram of the current flow in the parallel plate electrodes of a battery.

Table 1
Parameters for the electrodes

| Parameter | $Li_xC_6$ | $Li_yMn_2O_4$ |
|---|---|---|
| $S_{\mathrm{e}}$ ($\mathrm{S\,cm^{-1}}$) | 1.0 | 0.038 |
| $h_{\mathrm{e}}$ (μm) | 85 | 140 |
| $S_{\mathrm{c}}$ ($\mathrm{S\,cm^{-1}}$) | $6.33 \times 10^5$ | $3.83 \times 10^5$ |
| $h_{\mathrm{c}}$ (μm) | 10 | 20 |

polarization expression used by Tiedemann and Newman [16] and Newman and Tiedemann [9] was adopted

$$J = Y(V_p - V_n - U) \tag{12}$$

where $Y$ and $U$ are the fitting parameters. As suggested by Gu [17], $U$ and $Y$ were expressed as the following functions of the depth of discharge:

$$U = a_0 + a_1(\mathrm{DOD}) + a_2(\mathrm{DOD})^2 + a_3(\mathrm{DOD})^3 \tag{13}$$

$$Y = a_4 + a_5(\mathrm{DOD}) + a_6(\mathrm{DOD})^2 \tag{14}$$

where $a_0$–$a_6$ are the constants to be determined by experiments.

By solving the equations listed previously, the distribution of the current density, $J$, on the electrodes can be obtained as a function of the position on the electrode and the time. Therefore, DOD varies along with the position on the electrode and the time elapsed during discharge. The distribution of DOD on the electrode can be calculated from the distribution of $J$ as

$$\mathrm{DOD} = \frac{\int_0^t J\,\mathrm{d}t}{Q_T} \tag{15}$$

where $t$ is the discharge time (s) and $Q_T$ is the theoretical capacity per unit area (Ah cm$^{-2}$) of the electrodes. The uniformity index, UI, of DOD is defined as

$$\mathrm{UI} = \frac{\mathrm{DOD}_{max} - \mathrm{DOD}_{min}}{2\mathrm{DOD}_{avg}} \tag{16}$$

where $\mathrm{DOD}_{max}$, $\mathrm{DOD}_{min}$, and $\mathrm{DOD}_{avg}$ are the maximum, minimum, and average values of DOD on the electrodes, respectively. The lower the value of UI, the better the uniformity of DOD. Hence, a way to reduce UI should be devised in order to improve the uniformity of the utilization of the active material of the electrodes and to lengthen the life cycle of the battery.

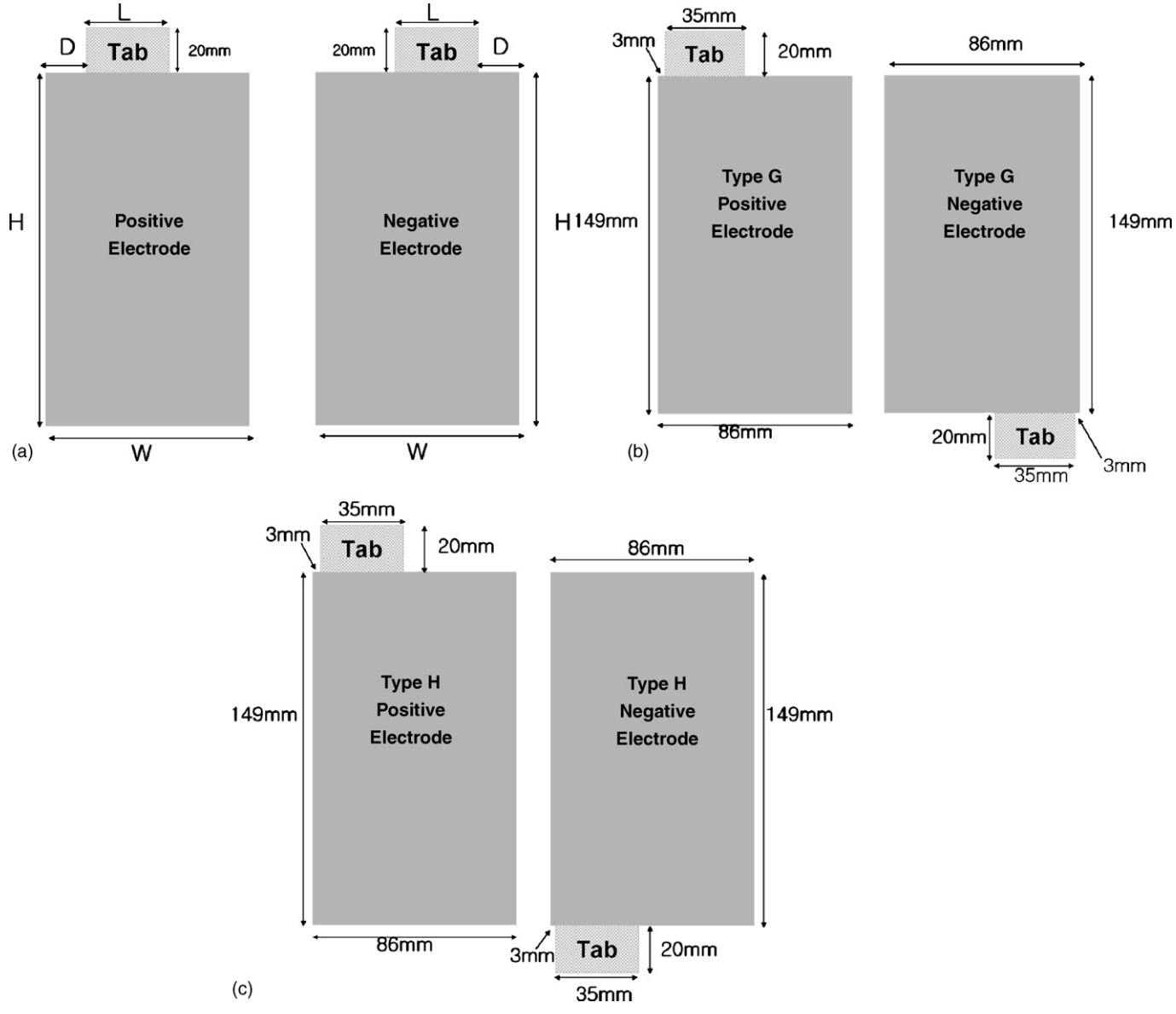


Fig. 2. Schematic diagrams of the electrode shapes for: (a) types A–F, (b) type G, and (c) type H.

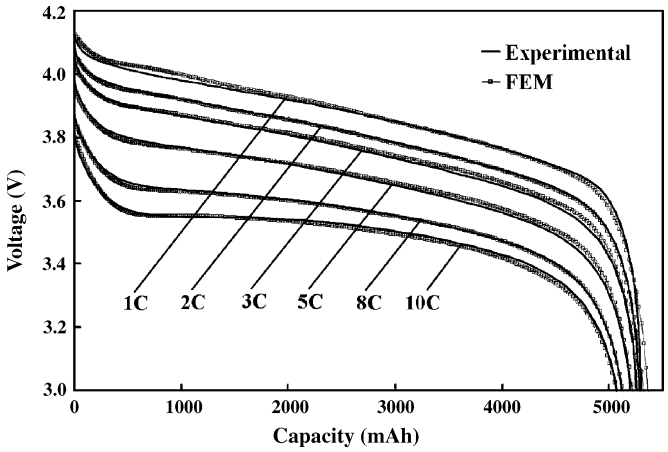


Fig. 3. Comparison between experimental and modeling discharge curves at discharge rates of 1*C*, 2*C*, 3*C*, 5*C*, 8*C*, and 10*C*. Solid lines are experimental data and lines with squares are modeling results based on the finite element method.

## 3. Results and discussion

The solutions to the governing Eqs. (5) and (6) subject to the associated boundary conditions (7)–(10) were obtained by using the finite element method. Numerical simulations were performed for the electrodes of eight different shapes of a lithium-polymer battery having a nominal capacity of 5 Ah. The electrodes of eight different shapes are referred to as the electrodes of types A–H. The schematic diagrams of the electrode shapes for types A–F, type G, and type H are illustrated in Fig. 2(a–c), respectively. The dimensions of the electrodes and the size and placing of current collecting tabs are listed in Table 2. In order to test the validity of the modeling, the calculated discharge curves based on modeling are compared with the experimental data in Fig. 3. The experiments were performed at room temperature by using the 5 Ah battery fabricated by VK Corporation with the electrodes of type A, of which the dimensions of the electrodes and the positions of the tabs

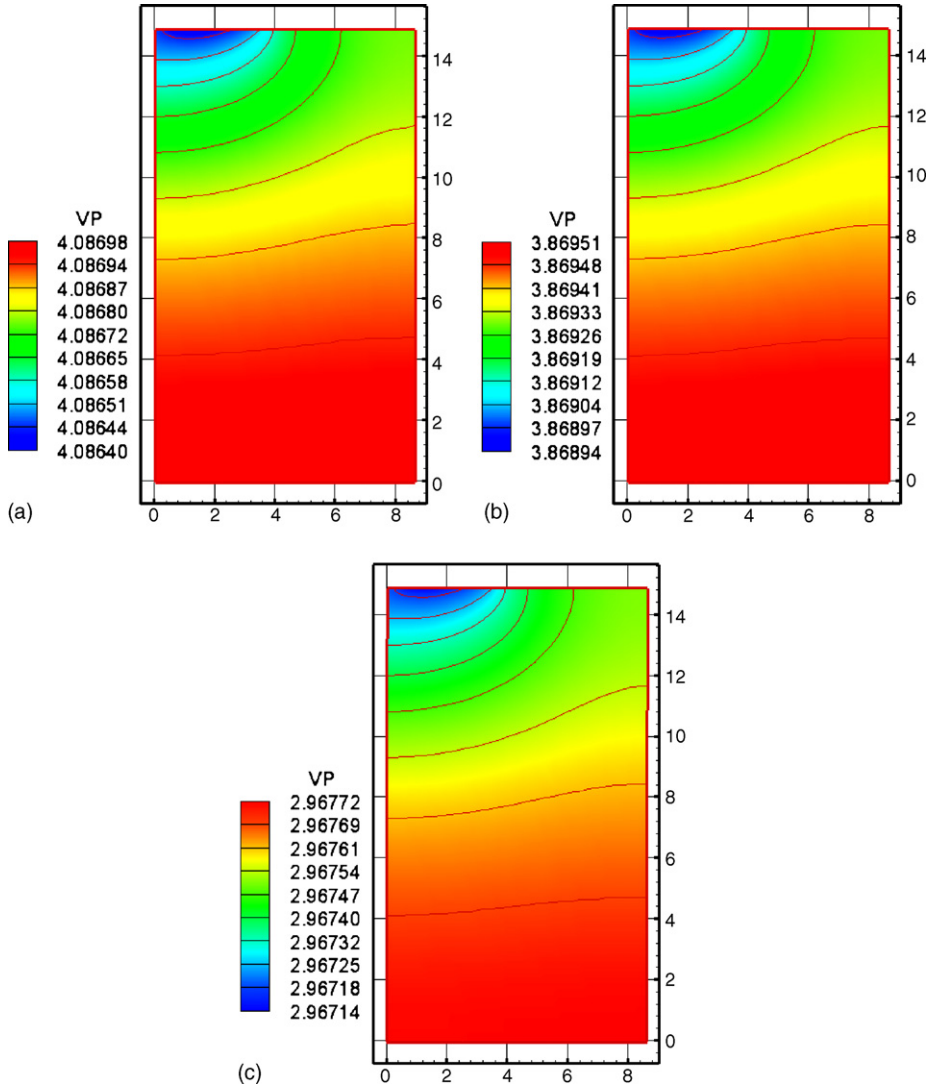


Fig. 4. Change of the distributions of potential on the positive electrode of type A during the discharge with 1*C* rate. Discharge times are: (a) 1 min, (b) 30 min, and (c) 59 min.

Table 2
Dimensions of the electrodes and the size and placing of current collecting tabs (unit: mm)

| | *W* | *H* | *D* | *L* |
|---|---|---|---|---|
| Type A | 86 | 149 | 3 | 35 |
| Type B | 149 | 86 | 3 | 35 |
| Type C | 113.2 | 113.2 | 3 | 35 |
| Type D | 86 | 149 | 3 | 18 |
| Type E | 86 | 149 | 25 | 35 |
| Type F | 86 | 149 | 34 | 18 |
| Type G | Refer to Fig. 2(b) | | | |
| Type H | Refer to Fig. 2(c) | | | |

are shown in Table 2 and Fig. 2(a). At various discharge rates from 1*C* to 10*C*, the experimental discharge curves are in good agreement with the modeling results based on the finite element method.

In Fig. 4, the change of the distributions of potential on the positive electrode of type A during the discharge with 1*C* rate is shown. The potential gradient is seen to be most severe in the region where the tab is attached to the current collector. This is because all the current flows through the conducting current collector into the tab from the entire electrode plate. Note that the values of the potential of Fig. 4(a–c) are around 4.09, 3.87, and 2.97 V, respectively. Although the appearances of the potential distribution are similar, the values of the potential at the beginning, in the middle, and at the end of discharge decrease complying with the discharge characteristics of the battery. In Fig. 5, only the distribution of potential on the negative

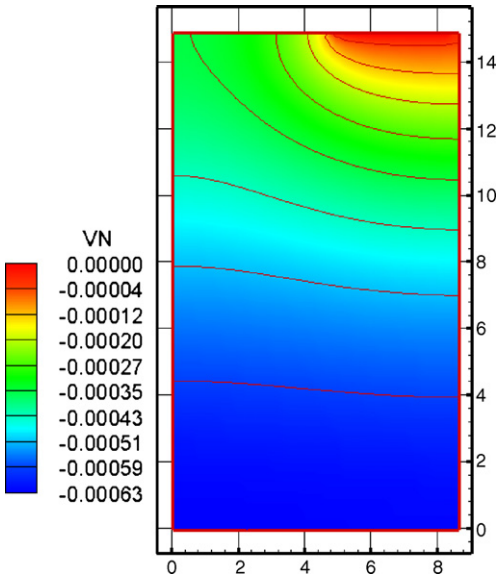


Fig. 5. Distribution of potential on the negative electrode of type A for the discharge rate of 1*C* at the discharge time of 1 min.

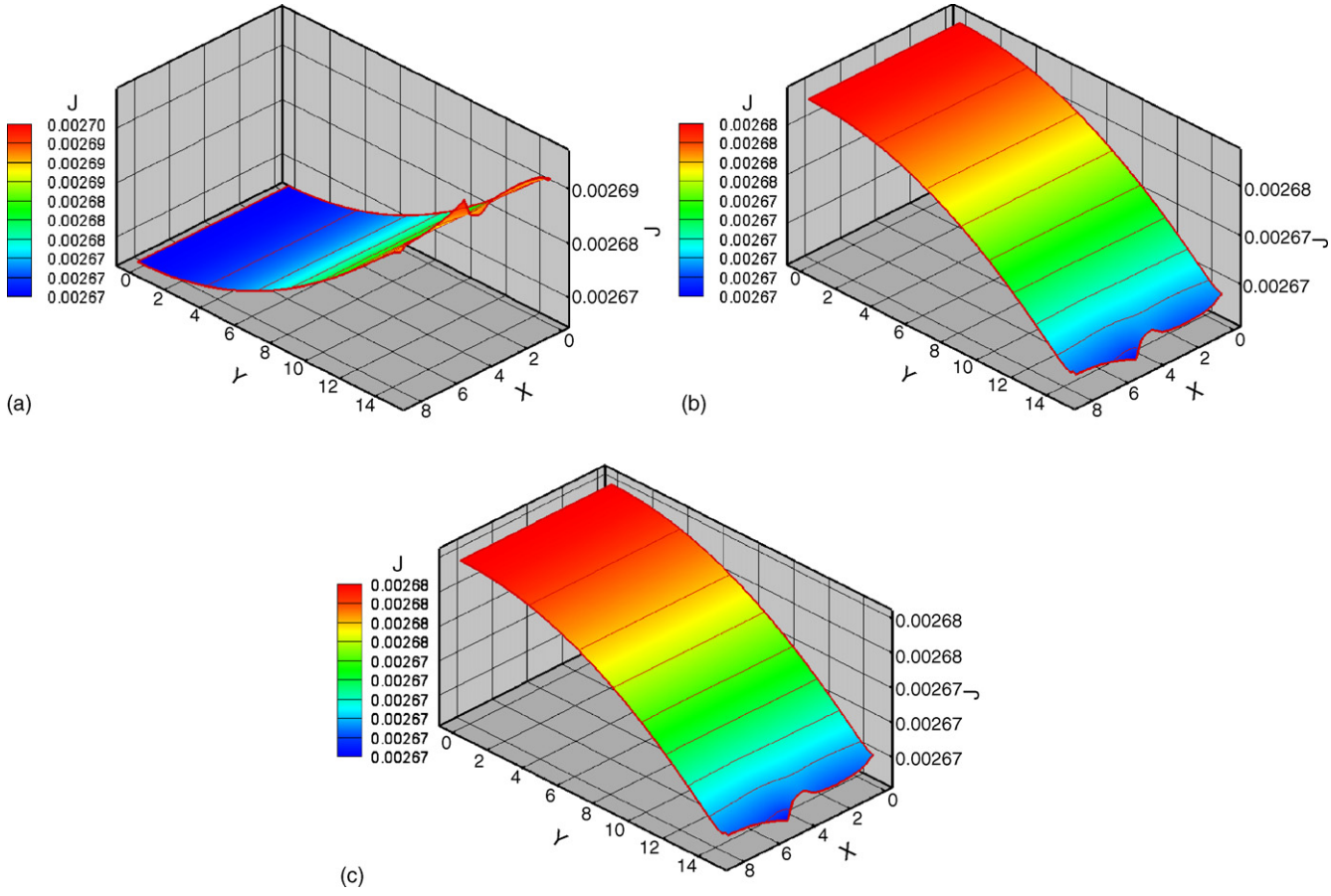


Fig. 6. Change of the distributions of current density transferred through the separator from the negative electrode to the positive electrode of type A during the discharge with 1*C* rate. Discharge times are: (a) 1 min, (b) 30 min, and (c) 59 min.

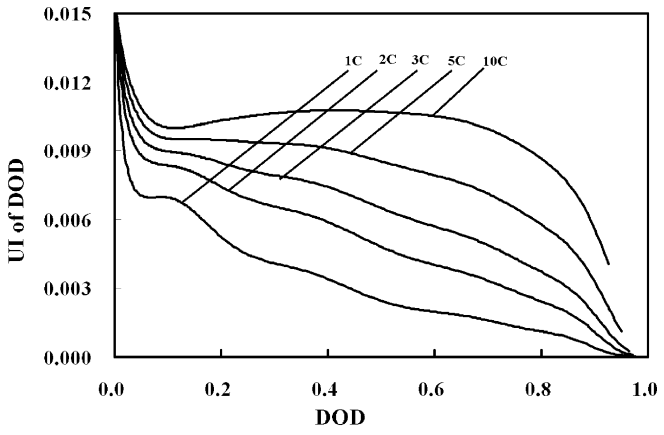


Fig. 7. UI of DOD of the electrode of type A as a function of the average DOD for the discharge rates of 1*C*, 2*C*, 3*C*, 5*C*, and 10*C*.

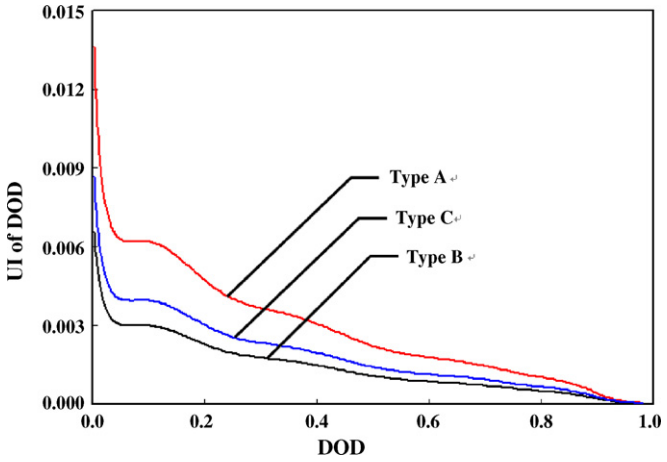


Fig. 8. UI's of DOD of the electrodes of types A–C as a function of the average DOD for the discharge rate of 1*C*.

electrode of type A at the discharge time of 1 min is shown, because the values of the potential and the appearances of the potential distribution on the negative electrode do not change according to the state of discharge. Again, the potential gradient is highest at the region near tab, because all the current has to flow from the tab through the entire electrode plate. Fig. 6 shows the change of the non-uniform distributions of current density transferred from the negative electrode to the positive electrode of type A during the discharge with 1*C* rate. At the initial stage of discharge (Fig. 6(a)), current density is higher in the region near the tabs than in the region distant from the tabs. However, after the midway stage of discharge (Fig. 6(b and c)), current density is lower in the region near the tabs than in the region distant from the tabs. This is because the less utilized region distant from the tabs becomes more favorable for reaction after the midway stage of discharge than the region near the tabs which is heavily utilized at the initial stage of discharge. A 'deformation' in the current density distribution at the upper center of the electrode observed in Fig. 6 may be due to the abrupt change of the directions of the current flow near the corners of the tabs of the positive and negative electrodes. The distributions of DOD on the electrodes can be obtained from the integration of the current density with time shown in Fig. 6. Although the DOD is higher in the region near the tabs than in the region distant from the tabs throughout the whole stages of discharge, the difference between the maximum and minimum values of DOD decreases as the discharge proceeds, since the reaction rate tends to be higher in the region where the active material is less utilized. This is reflected in the change of UI of DOD with time. At the initial stage of discharge, the value of UI of DOD is high, but it decreases as the discharge goes on. In Fig. 7, the UI of DOD for the discharge rates of 1*C*, 2*C*, 3*C*, 5*C*, and 10*C* are shown as a function of the average DOD over the entire electrode area. At all discharge rates, the UI of DOD decreases as average DOD increases. The UI of DOD maintains a higher value for a higher discharge rate than for a lower discharge rate throughout the whole stages of discharge. This trend illustrates that the non-uniformity of the utilization of the active material of electrodes becomes more pronounced at high discharge rates. Therefore, when the high discharge rates are repeated, there is a high chance that only a small fraction of electrode will be utilized excessively, thus reducing the life cycle of the battery.

To investigate the effect of the aspect ratio of the electrodes on the uniformity of the utilization of the active material of electrodes, the UI's of DOD for the electrodes of types A–C are shown as a function of the average DOD for the discharge rate of 1*C* in Fig. 8. It is assumed for the sake of modeling that the electrodes A–C have the same surface. In terms of the UI of DOD, the electrode of type B ($W > H$) has advantage over the electrode of type A ($W < H$) or the electrode of type C ($W = H$), where $W$ and $H$ denote the width and height of the electrode, respectively. In Fig. 9, the UI's of DOD of the electrodes of types A, D–G, and H are plotted as a function of the average DOD for the discharge rate of 1*C* in order to study the effect of the size and placing of current collecting tabs on the uniformity of the utilization of the active material of electrodes. This plot clearly shows which type of electrode is favorable in terms of the UI of DOD. From the plots of the UI of DOD of the types A and D, it can be deduced that the enlargement of the tab size

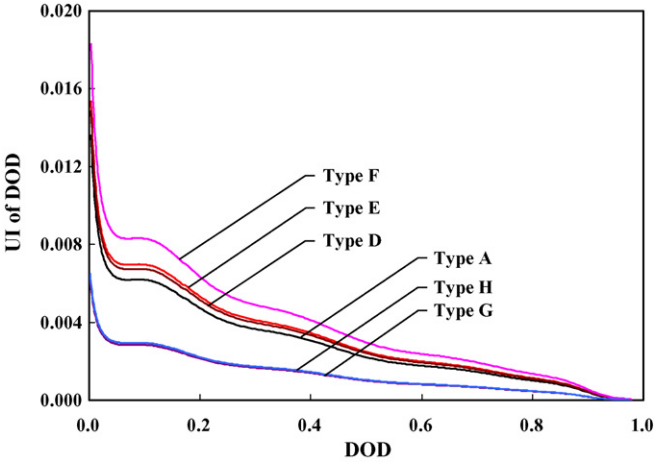


Fig. 9. UI's of DOD of the electrodes of types A, D–G, and H as a function of the average DOD for the discharge rate of 1*C*.

is favorable to the uniform utilization of active material. Based on the comparisons between the types A and E and between the types D and F, the reduction of the distance between the tabs is unfavorable for the cases investigated. As a major modification of the placing of tabs, the UI's of DOD as a function of the average DOD are calculated for the types H and G, where the tabs are on the opposing sides of a rectangular electrode. The electrodes of types H and G is more favorable than the others in terms of the UI of DOD. By the comparison between the types H and G, it can be noticed that placing the tabs diagonally is favorable, although the difference between the UI's of DOD of types H and G is minute.

## 4. Conclusions

A mathematical procedure was developed to study the potential and current density distribution on the electrodes for the scale-up of the electrode of a lithium-polymer battery. The distribution of the depth of discharge on the electrode was predicted as a function of discharge time from the calculated potential and current density distribution by using the finite element method. A quantitative examination was made of the effect of varying the configuration of the electrodes such as the aspect ratio of the electrodes and the size and placing of current collecting tabs as well as the discharge rates on the battery performance, in order to enhance the uniformity of the utilization of the active material of electrodes. The results showed that the aspect ratio of the electrodes and the size and placing of current collecting tabs have a significant effect on the potential and current density distribution on the electrodes to influence the DOD distribution on the electrodes, thus affecting the uniform utilization of the active material of electrodes. The methodology presented in this study, used to evaluate quantitatively the uniformity of the utilization of the active material of electrodes, should contribute to modifying the design of the electrode configuration.

## Acknowledgements

This work was supported by the Ministry of Commerce, Industry, and Energy of Republic of Korea under the Generic Technology Development Program. One of the authors (C.B. Shin) acknowledges the Korea Science and Engineering Foundation (KOSEF R01-2003-000-10103-0) and the FOI Corporation for providing partial financial supports for this work.

## References

[1] G. Cedar, M. Doyle, P. Arora, Y. Fuentes, MRS Bull. 27 (2002) 619–623.
[2] M. Doyle, T.F. Fuller, J. Newman, J. Electrochem. Soc. 140 (1993) 1526–1533.
[3] P. Arora, R.E. White, M. Doyle, J. Electrochem. Soc. 145 (1998) 3647–3667.
[4] G.G. Botte, V.R. Subramanian, R.E. White, Electrochim. Acta 45 (2000) 2595–2609.
[5] J. Newman, K.E. Thomas, H. Hafezi, D.R. Wheeler, J. Power Sources 119–121 (1990) 838–843.
[6] K.E. Thomas, R.M. Darling, J. Newman, Advances in Lithium-Ion Batteries, Kluwer Academic Publishers, New York, 2002, pp. 345–392.
[7] M.W. Verbrugge, J. Electrostat. 34 (1995) 61–85.
[8] D.R. Baker, M.W. Verbrugge, J. Electrochem. Soc. 146 (1999) 2413–2424.
[9] J. Newman, W. Tiedemann, J. Electrochem. Soc. 140 (1993) 1961–1968.
[10] G. Sikha, B.N. Popov, R.E. White, J. Electrochem. Soc. 151 (2004) A1104–A1114.
[11] G. Ning, B.N. Popov, J. Electrochem. Soc. 151 (2004) A1584–A1591.
[12] G. Ning, R.E. White, B.N. Popov, Electrochim. Acta 51 (2006) 2012–2022.
[13] D.W. Dees, V.S. Battaglia, A. Bélanger, J. Power Sources 110 (2002) 310–320.
[14] M. Doyle, J. Newman, A.S. Gozdz, C.N. Schmutz, J.-M. Tarascon, J. Electrochem. Soc. 143 (1996) 1890–1903.
[15] P. Arora, M. Doyle, A.S. Gozdz, R.E. White, J. Newman, J. Power Sources 88 (2000) 219–231.
[16] W. Tiedemann, J. Newman, in: S. Gross (Ed.), Battery Design and Optimization, The Electrochemical Society, Princeton, NJ, 1979, pp. 39–49.
[17] H. Gu, J. Electrochem. Soc. 130 (1983) 1459–1464.